

Contribution from the Research School of Chemistry, The Australian National University, Canberra, A.C.T. 2600, Australia, and the Department of Chemistry, Brandeis University, Waltham, Massachusetts 02154

Comparative Crystallography of Sterically Crowded Transition-Metal Complexes. 1. Structures of $[\text{Co}(\text{NH}_2\text{CH}_3)_5\text{Cl}](\text{NO}_3)_2$ and $[\text{Cr}(\text{NH}_2\text{CH}_3)_5\text{Cl}]\text{Cl}_2$

BRUCE M. FOXMAN¹

Received October 21, 1977

The crystal structures of the title complexes have been determined by single-crystal X-ray diffraction techniques. The cobalt complex crystallizes in space group $B\bar{1}$, with $a = 8.151(4) \text{ \AA}$, $b = 14.067(7) \text{ \AA}$, $c = 14.163(7) \text{ \AA}$, $\alpha = 106.78(10)^\circ$, $\beta = 93.45(10)^\circ$, and $\gamma = 89.56(10)^\circ$; block-diagonal least-squares refinement led to a conventional R value of 0.046 using 2068 reflections ($I > 3\sigma(I)$). The chromium complex is monoclinic, space group $P2_1/c$, $a = 11.537(5) \text{ \AA}$, $b = 8.134(3) \text{ \AA}$, $c = 15.191(6) \text{ \AA}$, and $\beta = 92.93(7)^\circ$, and full-matrix least-squares refinement of all 2365 reflections led to $R = 0.061$. Despite rather different packing arrangements, the configurations of the cobalt and chromium molecular cations are remarkably similar, lending credence to the hypothesis that observed distortions arise from intramolecular contacts. Both cations are severely distorted, with M-N-C and N-M-L angles deviating up to 15 and 6.6°, from "expected" tetrahedral and octahedral values, respectively. Further, inspection of intramolecular nonbonded contacts shows the cobalt complex to be considerably more strained. The structural data are in accord with the behavior of the complexes in simple octahedral substitution reactions. Thus, when methylamine is substituted for ammonia in $\text{M}(\text{NH}_3)_5\text{X}^{2+}$ (M = Co, Cr), kinetic steric effects are observed. The magnitude of the observed structural steric effects correlates well with (a) the magnitude of the observed kinetic steric effects and (b) the established mechanism for acid or base hydrolysis of chromium(III) and cobalt(III) amine and ammine complexes.

Introduction

A number of definitive papers in recent years have added greatly to the understanding of octahedral substitution processes in trivalent transition-metal ions, particularly those in the acidopentaammine and related classes.² In analogous series of complexes, there is an excellent opportunity for the assessment of the character of a substitution reaction: the study of kinetic steric effects—steric acceleration and steric retardation. Such studies have been carried out for $\text{Cr}(\text{NH}_2\text{R})_5\text{Cl}^{2+3}$ and $\text{Co}(\text{NH}_2\text{R})_5\text{Cl}^{2+4}$ where R = H or alkyl. The results of these studies indicated that these species undergo acid hydrolysis by an I_a and I_d mechanism, respectively. In the case of base hydrolysis both compounds show steric acceleration (characteristic of an I_d or D process) as R is varied from H to CH_3 ; however, the kinetic steric effect is much less spectacular for complexes of Cr (225) than for those of Co (~15 000). On the basis of measurements of ΔH^* , ΔS^* , and ΔV^* for a large number of octahedral substitution reactions, and the results of a structure determination on $[\text{Co}(\text{NH}_2\text{C}-\text{H}_3)_5\text{Cl}](\text{NO}_3)_2$ carried out by us,⁵ Swaddle and co-workers⁶ have pointed out (a) "that, of the trivalent transition metal ions, only cobalt(III) forms cationic complexes which react by I_d mechanisms in simple substitution reactions" and (b) that steric compression in the ground state of octahedral complexes would greatly facilitate I_d processes, while rendering I_a processes energetically inaccessible.

We report here the crystal and molecular structures of $[\text{Co}(\text{NH}_2\text{CH}_3)_5\text{Cl}](\text{NO}_3)_2$ and $[\text{Cr}(\text{NH}_2\text{CH}_3)_5\text{Cl}]\text{Cl}_2$, which represent a quantitative comment on our earlier ideas^{4,5} and on the postulates of Swaddle et al.⁶ Our purpose in making this comparative crystallographic study was twofold: (a) Cr(III)-N bonds are ~0.1 Å longer than Co(III)-N bonds, hence it is possible to obtain correlations between "structural distortions" and differences in mechanistic behavior between Co and Cr complexes; (b) since the two cations crystallize in different packing arrangements, any similarities between them should be attributable to common intramolecular effects.

Experimental Section

$[\text{Co}(\text{NH}_2\text{CH}_3)_5\text{Cl}](\text{NO}_3)_2$ Crystal Data. $[\text{Co}(\text{NH}_2\text{CH}_3)_5\text{Cl}]\text{Cl}_2$ was prepared as described previously;⁴ however, crystals of this complex proved to be unsuitable for X-ray studies due to twinning. Suitable crystals of the corresponding nitrate salt were readily obtained by recrystallization of the chloride salt from HNO_3 -water mixtures. Weissenberg ($0kl$, $1kl$) and precession ($h0l$, $h1l$, $hk0$, $hk1$) photographs

established that the crystal belonged to the triclinic system; the observed systematic absences, hkl , $h + l = 2n + 1$, indicated that the space group was $B\bar{1}$ or $B\bar{1}$, nonstandard settings of $P\bar{1}$ or $P\bar{1}$, respectively.⁷ Initially, $B\bar{1}$ was selected as the likely space group, and subsequent refinement of the structure supports this choice.

The crystal, of dimensions $0.10 \times 0.175 \times 0.475 \text{ mm}$ (elongated along a), with well-defined $\{110\}$, $\{012\}$, $\{010\}$, and $\{001\}$ faces, was transferred to a Picker FACS-I diffractometer and aligned such that the crystallographic a axis was approximately coincident with the φ axis of the goniostat. Unit cell parameters at $21(1)^\circ$, derived from least-squares refinement⁸ of the observed values for 2θ , ω , φ , and χ for 12 high-order reflections ($74 < 2\theta < 103^\circ$), measured at a takeoff angle of 3° , were found to be $a = 8.151(4) \text{ \AA}$, $b = 14.067(7) \text{ \AA}$, $c = 14.163(7) \text{ \AA}$, $\alpha = 106.78(10)^\circ$, $\beta = 93.45(10)^\circ$, $\gamma = 89.56(10)^\circ$, and λ (Cu $K\alpha_1$) 1.54051 \AA . The values quoted above were constant for four separate determinations during data collection; the quoted errors represent a conservative estimate of the precision of cell constant measurements. The corresponding primitive, Delaunay reduced cell has $a = 14.481 \text{ \AA}$, $b = 14.067 \text{ \AA}$, $c = 8.151 \text{ \AA}$, $\alpha = 90.44^\circ$, $\beta = 107.66^\circ$, and $\gamma = 145.90^\circ$. The observed density, $1.60(1) \text{ g cm}^{-3}$, measured by flotation in $\text{CCl}_4\text{-CH}_2\text{I}$ agrees well with the calculated value of 1.599 g cm^{-3} for $Z = 4$ in $B\bar{1}$. The structure was solved and refined in terms of the nonreduced cell, and the subsequent atomic positional parameters refer to this cell.

Data Collection. Graphite crystal-monochromated Cu $K\alpha$ radiation (takeoff angle = 3°) was used to collect 2914 reflections, including "check" reflections, of the type $h\bar{k}l$, $\bar{h}kl$, hkl , and $\bar{h}kl$ within the sphere bounded by $(\sin \theta)/\lambda \leq 0.575$. The θ - 2θ scan mode was used, with a 2θ scan speed of $2^\circ/\text{min}$, and a scan range from 1.0° in 2θ below the Cu $K\alpha_1$ peak to 1.0° in 2θ above the Cu $K\alpha_2$ peak. The pulse height analyzer was set to admit 95% of the Cu $K\alpha$ peak, and the counter was 30 cm from the crystal. Backgrounds were measured for 10 s each at the scan range limits. Three standard reflections ($\bar{1}, \bar{1}, 11$, $\bar{6}50$, $\bar{4}, 12, 0$) were monitored after each 40 reflections had been measured. These showed a steady decrease with time, of a total of 8.7, 11.3, and 15.2%, respectively. An isotropic exponential decay correction, with allowance for $(\sin \theta)/\lambda$ dependence,⁹ was applied to the entire data set. Attenuators were nonfunctional during data collection; the intensities of the 15 most intense reflections were remeasured at a lower applied power. Eight of these had counting rates during data collection which exceeded the linear range of the counter and were rescaled.

Data were reduced to values of $|F_o|$ using the program SETUP.¹⁰ The Lorentz-polarization factor is given by $LP = (\cos^2 2\theta + \cos^2 2\theta_m)/[\sin 2\theta(1 + \cos^2 2\theta_m)]$ where $2\theta_m = 26.50^\circ$ is the Bragg angle for the monochromator. The derived structure amplitudes were each assigned standard deviations

$$\sigma(F_o) = [(\sigma(I)/LP)^2 + (\rho|F_o|^2)^2]^{1/2}/2|F_o|$$

where $\sigma(I) = [CT + (t_p/t_b)^2(B_1 + B_2)]^{1/2}$, CT is the integrated peak intensity counted for t_p seconds, B_1 and B_2 are the individual background counts, each counted for $t_b/2$ seconds, and $\rho = 0.032$ is the instrumental "uncertainty" factor.¹¹ The data were sorted, and averaging of equivalent forms was performed by the program SORTIE.¹⁰ Those reflections for which $I/\sigma(I) \leq 3.0$ (where $I = [CT - (t_p/t_b)(B_1 + B_2)]$) were rejected as unobserved. The statistical R factor, $R_s(F_o)$, for the 2068 reflections (84% of the number theoretically possible) in the final data set is 0.018. ($R_s(F_o) = \sum \sigma_s(F_o) / \sum |F_o|$, and $\sigma_s(F_o) = \sigma(I)/2(LP)(|F_o|)$.)

Solution and Refinement of the Structure. The positions of the Co, Cl, and five methylamine N atoms were obtained from a three-dimensional Patterson map; the remaining nonhydrogen atoms were obtained from a difference Fourier synthesis following the first structure-factor calculation. Three cycles of full-matrix least-squares refinement, varying scale factor, positional parameters, and individual isotropic temperature factors for all atoms, converged with $R = 0.110$ and $R_w = 0.120$ (unit weights).¹² Since further refinement was restricted by storage limitations and, to a certain extent, cost factors, the local (CDC 3600) version of Prewitt's SFLS-5 was modified to include block-diagonal refinement.^{10,13} Testing of this program with several data sets indicated that the standard deviations obtained from 4×4 matrices of x , y , z , and B for individual atoms were almost identical (for this particular structure, within $\sim 2\%$) with those obtained from inversion of the full matrix. At this point, corrections for anomalous scattering were introduced^{14a} for Co and Cl,^{14b} and each atom was assigned individual anisotropic temperature factors (suggested by features on a difference map), and refinement converged after four cycles, with $R = 0.073$ and $R_w = 0.088$.

The intensity data were corrected for absorption effects (ACACA¹⁰) ($\mu = 108.6 \text{ cm}^{-1}$), using a grid of $4 \times 6 \times 10$ points parallel to b^* , c , and a , respectively. Transmission factors varied from 0.142 to 0.413. Three cycles of further refinement using absorption-corrected data resulted in convergence, with $R = 0.061$ and $R_w = 0.082$ ($w = 1/\sigma^2(F_o)$ for this and further refinement).

A difference Fourier synthesis at this point revealed the approximate positions of the 25 hydrogen atoms. These were not used directly but were used in the following manner to determine calculated positions for the hydrogen atoms. The program CONTACT¹⁰ was used to generate "tetrahedral" positions for the amine protons and also to generate positions for methyl H atoms at 5° intervals about the N-C bond axis. Calculated H atom positions were then selected, which were the "best fit" to a given set of three observed proton positions. ($r_{N-H} = 1.01 \text{ \AA}$; $r_{C-H} = 1.08 \text{ \AA}$).¹⁵ The hydrogen atoms were included, as fixed contributions to F_o , in subsequent cycles of least-squares refinement; the calculation procedure above was repeated after each cycle of refinement. Four further cycles of least-squares refinement converged with $R = 0.046$ and $R_w = 0.056$. On the final cycle, no individual parameter shift was greater than 0.07 of the corresponding esd.

A final difference Fourier map showed a peak of 0.5 e/\AA^3 near the Cl atom and no other maxima greater than 0.3 e/\AA^3 . Further refinement was attempted in which a secondary extinction correction was applied,¹⁶ but since no decrease in R or R_w resulted, this stage of refinement was abandoned. A weighting scheme analysis revealed no serious dependence of $w[|F_o| - |F_c|]^2$ on either $|F_o|$ or $(\sin \theta)/\lambda$. The standard deviation of an observation of unit weight, defined as $\{\sum w[|F_o| - |F_c|]^2 / (m - n)\}^{1/2}$ (where $m (=2068)$ is the number of observations and $n (=181)$ is the number of parameters varied) is 2.46. Final atomic coordinates and thermal parameters, U_{ij} , together with their estimated standard deviations (where appropriate) are listed in Tables I and II, respectively.

[Cr(NH₂CH₃)₅Cl] Crystal Data. The chloride salt was prepared as described by Rogers and Staples.¹⁷ Weissenberg ($hk0$, $hk1$) photographs established that the crystal belonged to the monoclinic system; the observed systematic absences, $h0l$, $l = 2n + 1$, and $0k0$, $k = 2n + 1$, are consistent only with space group $P2_1/c$ (No. 14). However, it was noted that most of the $hk0$ reflections for which $h + k$ was odd (all except a very faint 500!) were absent. Laué photographs of the crystal (Mo unfiltered radiation) indicated it to be of excellent quality. Thus it was decided to proceed with the data collection, assuming that the unusual absences were induced due to pseudospecial positioning (e.g., Cr at $(1/4, 1/4, z)$ or $(1/4, 0, z)$) of the molecule, rather than some effect due to twinning. (Our concern here arose because of the twinning problem encountered with the chloride salt of the analogous cobalt complex.) The prismatic crystal

Table I. Atomic Coordinates and Isotropic Temperature Factors for [Co(NH₂CH₃)₅Cl](NO₃)₂^a

Atom	x	y	z
Co	0.06030 (8)	0.22906 (5)	0.25217 (5)
Cl	0.11311 (17)	0.16964 (10)	0.38473 (9)
N1	0.00402 (41)	0.27352 (24)	0.13382 (23)
C1	0.09291 (58)	0.35656 (34)	0.11651 (33)
N2	0.18551 (45)	0.11355 (26)	0.17347 (27)
C2	0.31002 (56)	0.12330 (37)	0.10494 (35)
N3	0.27313 (43)	0.30262 (25)	0.29022 (25)
C3	0.29530 (59)	0.38786 (35)	0.38066 (35)
N4	-0.06979 (43)	0.34314 (25)	0.32521 (24)
C4	-0.11060 (66)	0.36062 (37)	0.42935 (33)
N5	-0.14079 (45)	0.14346 (27)	0.22632 (27)
C5	-0.23494 (57)	0.10986 (35)	0.13011 (34)
N6	0.59920 (45)	0.39980 (26)	0.17632 (26)
O1	0.71887 (42)	0.42446 (29)	0.14053 (27)
O2	0.46803 (39)	0.44540 (24)	0.17773 (25)
O3	0.60812 (45)	0.32907 (25)	0.21238 (30)
N7	0.52546 (44)	0.12002 (26)	0.37559 (26)
O4	0.50527 (47)	0.06593 (25)	0.28878 (22)
O5	0.56336 (50)	0.20763 (25)	0.39257 (30)
O6	0.50147 (43)	0.08390 (25)	0.44486 (22)

Atom	x	y	z	$U, \text{ \AA}^2$
H1N1	0.0189	0.2141	0.0746	0.0465
H2N1	-0.1158	0.2922	0.1364	0.0465
H1N2	0.2444	0.0841	0.2231	0.0590
H2N2	0.1005	0.0647	0.1324	0.0590
H1N3	0.3583	0.2521	0.2972	0.0515
H2N3	0.2983	0.3286	0.2332	0.0515
H1N4	-0.0082	0.4045	0.3232	0.0523
H2N4	-0.1786	0.3385	0.2860	0.0523
H1N5	-0.1065	0.0810	0.2434	0.0567
H2N5	-0.2215	0.1809	0.2748	0.0567
H1C1	0.0378	0.3736	0.0523	0.0600
H2C1	0.0871	0.4209	0.1798	0.0600
H3C1	0.2195	0.3368	0.1046	0.0600
H1C2	0.3295	0.0518	0.0528	0.0654
H2C2	0.2673	0.1750	0.0655	0.0654
H3C2	0.4242	0.1505	0.1464	0.0654
H1C3	0.2252	0.4500	0.3708	0.0647
H2C3	0.2526	0.3670	0.4428	0.0647
H3C3	0.4238	0.4081	0.3943	0.0647
H1C4	-0.1995	0.4194	0.4482	0.0685
H2C4	-0.1612	0.2934	0.4387	0.0685
H3C4	-0.0004	0.3819	0.4771	0.0685
H1C5	-0.1522	0.0782	0.0728	0.0618
H2C5	-0.3245	0.0544	0.1324	0.0618
H3C5	-0.2974	0.1722	0.1148	0.0618

^a Standard deviations in the least significant digit appear in parentheses in this and subsequent tables.

used for data collection was mounted on a quartz fiber and had approximate dimensions $0.09 \times 0.19 \times 0.29 \text{ mm}$. It was transferred to a Syntex $P2_1$ diffractometer and centered optically using a Supper No. 455 goniometer. Since this work is the first structural study completed in this research group using the Syntex diffractometer,¹⁸ we describe our experimental procedure in detail for future reference.

(1) A normal-beam, flat-film rotation photograph¹⁹ was taken with $2\theta = \omega = \chi = 0^\circ$ with the φ axis rotating at $234^\circ/\text{min}$ for 20 min. A Polaroid film cassette was mounted on the detector arm, approximately 9.7 cm from the crystal.

(2) Fifteen reflections were chosen from this photograph and located and centered by an automatic routine. The refined 2θ , ω , φ , and χ values were used as input to an autoindexing routine, and a cell and indices consistent with the Weissenberg photographs were assigned. Least-squares refinement of these reflections gave an orientation matrix and a set of "starting" cell constants.

(3) The information in step (2) was used to collect all independent data rapidly in the 2θ range $24\text{--}27^\circ$. From these, 12 strong reflections, well dispersed in reciprocal space, were automatically centered. The refined angular values were used in least-squares refinement of cell parameters and orientation matrix for data collection (Mo $K\alpha$ used).

(4) $\theta\text{--}2\theta$ and ω scans, displayed as line-printer plots, showed the crystal to be acceptable (in agreement with the more comprehensive Laué photographs).

Table II. Anisotropic Thermal Parameters for $[\text{Co}(\text{NH}_2\text{CH}_2)_3\text{Cl}](\text{NO}_3)_2^a$

Atom	U_{11}	U_{22}	U_{33}	U_{12}	U_{13}	U_{23}
Co	0.02790 (34)	0.03657 (33)	0.03434 (32)	-0.00161 (26)	0.00418 (26)	0.00923 (27)
Cl	0.06247 (84)	0.06624 (81)	0.05522 (71)	0.00167 (64)	-0.00078 (60)	0.02752 (62)
N1	0.0313 (20)	0.0378 (19)	0.0355 (19)	0.0016 (16)	0.0072 (15)	0.0097 (16)
C1	0.0442 (29)	0.0561 (29)	0.0458 (26)	-0.0066 (23)	0.0079 (22)	0.0193 (22)
N2	0.0378 (22)	0.0421 (22)	0.0529 (23)	0.0034 (17)	0.0018 (18)	0.0075 (18)
C2	0.0327 (27)	0.0652 (32)	0.0510 (29)	0.0062 (23)	0.0066 (22)	0.0028 (24)
N3	0.0329 (21)	0.0434 (21)	0.0401 (19)	-0.0022 (17)	0.0012 (16)	0.0103 (17)
C3	0.0421 (29)	0.0523 (29)	0.0533 (29)	-0.0038 (23)	-0.0051 (23)	0.0050 (23)
N4	0.0381 (22)	0.0455 (22)	0.0362 (19)	0.0031 (17)	0.0104 (16)	0.0072 (17)
C4	0.0637 (35)	0.0617 (32)	0.0400 (26)	-0.0008 (26)	0.0176 (25)	0.0078 (23)
N5	0.0372 (22)	0.0476 (22)	0.0486 (22)	-0.0073 (17)	0.0082 (17)	0.0135 (18)
C5	0.0360 (27)	0.0539 (29)	0.0517 (29)	-0.0046 (22)	0.0079 (22)	0.0060 (23)
N6	0.0383 (22)	0.0436 (21)	0.0426 (20)	0.0011 (17)	-0.0006 (17)	0.0052 (17)
O1	0.0407 (21)	0.0958 (28)	0.0800 (26)	0.0002 (19)	0.0189 (19)	0.0368 (22)
O2	0.0379 (20)	0.0619 (22)	0.0697 (23)	0.0091 (16)	0.0030 (17)	0.0187 (18)
O3	0.0571 (25)	0.0518 (22)	0.1138 (32)	-0.0020 (18)	-0.0040 (22)	0.0389 (21)
N7	0.0374 (22)	0.0427 (21)	0.0464 (21)	0.0023 (17)	0.0035 (17)	0.0136 (18)
O4	0.0799 (27)	0.0654 (23)	0.0369 (18)	-0.0022 (19)	0.0063 (17)	0.0122 (16)
O5	0.0869 (31)	0.0408 (20)	0.1020 (31)	-0.0150 (19)	0.0036 (24)	0.0204 (20)
O6	0.0654 (24)	0.0645 (22)	0.0427 (19)	-0.0012 (18)	0.0078 (16)	0.0238 (17)

^a The form of the thermal ellipsoid in this table and Table IV is $\exp[-2\pi^2(a^{*2}U_{11}h^2 + \dots + 2b^*c^*U_{23}kl)]$.

Table III. Atomic Coordinates and Isotropic Temperature Factors for $[\text{Cr}(\text{NH}_2\text{CH}_2)_3\text{Cl}]\text{Cl}_2$

Atom	<i>x</i>	<i>y</i>	<i>z</i>	<i>U</i> , Å ²
Cr	0.25096 (5)	0.25274 (7)	0.10845 (4)	
Cl1	0.25432 (9)	0.03279 (13)	0.01359 (7)	
Cl2	0.51719 (9)	0.64063 (14)	0.15082 (7)	
Cl3	-0.02043 (9)	0.63881 (14)	0.13637 (7)	
N1	0.24556 (34)	0.46765 (44)	0.18517 (23)	
N2	0.07143 (31)	0.26904 (50)	0.08190 (29)	
N3	0.23759 (39)	0.10448 (45)	0.22104 (25)	
N4	0.43028 (32)	0.25697 (49)	0.13646 (30)	
N5	0.26743 (40)	0.39820 (46)	-0.00436 (25)	
C1	0.24344 (56)	0.46140 (67)	0.28118 (33)	
C2	-0.00529 (44)	0.14296 (81)	0.11306 (44)	
C3	0.24394 (59)	-0.07793 (58)	0.21555 (41)	
C4	0.50878 (45)	0.15122 (73)	0.09005 (43)	
C5	0.25703 (55)	0.57857 (62)	-0.00619 (36)	
H1N1	0.192 (3)	0.514 (5)	0.164 (2)	0.0140 (8)
H2N1	0.317 (4)	0.527 (6)	0.173 (3)	0.0407 (9)
H1N2	0.062 (6)	0.255 (8)	0.020 (5)	0.0939 (19)
H2N2	0.055 (7)	0.339 (10)	0.113 (5)	0.1269 (26)
H1N3	0.185 (4)	0.126 (6)	0.242 (3)	0.0470 (13)
H2N3	0.303 (5)	0.141 (6)	0.254 (3)	0.0549 (12)
H1N4	0.450 (5)	0.245 (7)	0.201 (4)	0.0844 (16)
H2N4	0.449 (4)	0.356 (6)	0.128 (3)	0.0428 (11)
H1N5	0.216 (6)	0.360 (8)	-0.044 (4)	0.0951 (19)
H2N5	0.345 (6)	0.365 (9)	-0.026 (4)	0.1149 (20)
H1C1	0.188 (4)	0.419 (5)	0.292 (3)	0.0225 (10)
H2C1	0.327 (6)	0.406 (9)	0.305 (4)	0.1082 (18)
H3C1	0.246 (5)	0.572 (8)	0.305 (4)	0.0767 (14)
H1C2	-0.075 (4)	0.143 (5)	0.086 (3)	0.0404 (9)
H2C2	0.033 (4)	0.023 (7)	0.107 (3)	0.0677 (13)
H3C2	-0.001 (7)	0.161 (11)	0.179 (5)	0.1313 (23)
H1C3	0.329 (5)	-0.099 (7)	0.190 (4)	0.0803 (14)
H2C3	0.196 (6)	-0.112 (8)	0.172 (4)	0.0907 (17)
H3C3	0.247 (5)	-0.132 (8)	0.265 (4)	0.0829 (16)
H1C4	0.580 (5)	0.175 (6)	0.112 (3)	0.0476 (10)
H2C4	0.489 (5)	0.197 (8)	0.030 (4)	0.0815 (15)
H3C4	0.488 (4)	0.037 (8)	0.106 (3)	0.0694 (13)
H1C5	0.280 (5)	0.603 (7)	-0.064 (4)	0.0727 (13)
H2C5	0.335 (6)	0.614 (8)	0.034 (4)	0.0911 (15)
H3C5	0.195 (5)	0.602 (6)	0.016 (3)	0.0508 (12)

(5) The intensities of 3194 reflections, including check reflections, of the type hkl and $hk\bar{l}$, within the sphere bounded by $(\sin \theta)/\lambda < 0.618$, were measured using the θ - 2θ scan technique. The scan range was from 1.0° in 2θ below the $K\alpha_1$ peak to 1.0° above the $K\alpha_2$ peak. The scan rate was varied from 1.46 to $11.72^\circ/\text{min}$. The pulse height analyzer was set to admit 95% of the Mo $K\alpha$ peak, and the counter was 30 cm from the crystal. Backgrounds were measured for 0.25

of the total scan time at each of the scan range limits. Any step of the scan which exceeded 5000 counts/s was subjected to a standard correction for coincidence losses¹⁸ ($I_{\text{true}} = I_{\text{obsd}} + \tau I_{\text{true}}^2$; $\tau = 2.6 \times 10^{-6}$). The "dead time", τ , and the maximum count rate to which the correction applies (60000 counts/s) were determined experimentally for our configuration. Four standard reflections (10,0,10, 080, 321, 018) were monitored after measurement of each 38 reflections. Each of these varied by less than $\pm 3\sigma(I)$ from its mean throughout data collection. None of the measured intensities exceeded the linear range of the counter.

(6) At the end of data collection, the list was scanned, and intense high-order reflections were chosen for a cell constant determination. Unit cell parameters at $23 (1)^\circ$, using the 2θ , ω , φ , and χ values of $15 \pm 2\theta$ reflections ($42 < |2\theta| < 52^\circ$) were found to be $a = 11.537 (5) \text{ \AA}$, $b = 8.134 (3) \text{ \AA}$, $c = 15.191 (6) \text{ \AA}$, $\beta = 92.93 (7)^\circ$, and $\lambda(\text{Mo } K\alpha_1) = 0.70926 \text{ \AA}$. The cell constant determination procedure was checked using (a) a very small crystal of $\text{Pb}(\text{NO}_3)_2$ ²⁰ and (b) a crystal of $[\text{Co}(\text{NH}_2\text{CH}_2)_3\text{Cl}](\text{NO}_3)_2$. The values obtained were in good agreement (differences < 1 standard deviation) with published values or values obtained on the A.N.U. Picker diffractometer described above. Further, these values were in excellent agreement with the Mo $K\alpha$ cell constant values obtained in step (3) above. The observed density, $1.46 (1) \text{ g cm}^{-3}$, measured by flotation in CHCl_3 -EtOH, agrees well with the calculated value of 1.464 g cm^{-3} for $Z = 4$.

Solution and Refinement of the Structure. Initial calculations were performed on a CDC 6400 computer at Smithsonian Astrophysical Observatory, Cambridge, Mass., and on an IBM 370 system at the MIT Computation Center, using locally modified versions of the programs described previously.¹⁰ The analysis was completed some time later on a Syntex XTL structure determination system, consisting of a NOVA 1200 computer (24 K of 16-bit memory), a 1.2 million word Diablo disk unit, and a Versatec D1100A printer/plotter. All final results and drawings reported here were obtained using the XTL system.²¹

The quantities I and $\sigma(I)$ were computed as described above, except that here, for $I < 0.7\sigma(I)$, the intensity was set equal to $0.7\sigma(I)$. The stochastic R factor, $R_s(F_o)$, for the 1723 reflections (73% of the total measured) with $I > 1.96\sigma(I)$, was 0.031; however, no reflections were rejected as unobserved, and all 2365 reflections were used in the final data set. Each $|F_o|$ was assigned a standard deviation $\sigma(F_o) = \sigma(I)/2(LP)(|F_o|)$, where

$$LP = \frac{0.5}{\sin 2\theta} \left[\left(\frac{1 + (\cos^2 2\theta_M)(\cos^2 2\theta)}{1 + \cos^2 2\theta_M} \right) + \left(\frac{1 + |\cos 2\theta_M|(\cos^2 2\theta)}{1 + |\cos 2\theta_M|} \right) \right]$$

This expression for the LP factor for a monochromator in the parallel

Table IV. Anisotropic Thermal Parameters for $[\text{Cr}(\text{NH}_2\text{CH}_3)_5\text{Cl}]_2$

Atom	U_{11}	U_{22}	U_{33}	U_{12}	U_{13}	U_{23}
Cr	0.01971 (33)	0.02355 (33)	0.02711 (32)	-0.00028 (23)	0.00134 (23)	-0.00093 (24)
Cl1	0.04368 (61)	0.03906 (56)	0.04163 (57)	0.00044 (51)	0.00268 (46)	-0.01338 (46)
Cl2	0.03804 (58)	0.04372 (61)	0.04996 (65)	-0.00728 (51)	-0.00131 (48)	-0.00237 (49)
Cl3	0.03797 (58)	0.04688 (63)	0.04473 (60)	0.00630 (51)	0.00300 (46)	-0.00090 (50)
N1	0.0293 (20)	0.0287 (18)	0.0416 (20)	0.0034 (18)	-0.0030 (17)	-0.0001 (15)
N2	0.0262 (19)	0.0430 (23)	0.0454 (23)	-0.0021 (17)	0.0037 (16)	-0.0030 (19)
N3	0.0343 (22)	0.0314 (20)	0.0405 (21)	-0.0023 (18)	0.0028 (19)	0.0019 (16)
N4	0.0308 (20)	0.0289 (21)	0.0651 (28)	-0.0006 (17)	0.0013 (18)	-0.0044 (19)
N5	0.0495 (24)	0.0373 (21)	0.0380 (21)	0.0018 (19)	0.0057 (19)	0.0062 (17)
C1	0.0547 (34)	0.0354 (27)	0.0471 (28)	-0.0013 (27)	0.0079 (25)	-0.0112 (23)
C2	0.0257 (26)	0.0717 (41)	0.0776 (41)	-0.0156 (27)	-0.0066 (25)	0.0142 (31)
C3	0.0803 (42)	0.0284 (25)	0.0535 (32)	-0.0046 (26)	-0.0049 (31)	0.0091 (23)
C4	0.0299 (27)	0.0518 (33)	0.0787 (41)	0.0068 (25)	0.0052 (26)	-0.0026 (29)
C5	0.0587 (35)	0.0448 (29)	0.0442 (29)	-0.0035 (26)	0.0087 (27)	0.0120 (23)

mode assumes the monochromator crystal to be 50% mosaic and 50% perfect.

Trial positions for Cr, 3Cl, and 5N atoms were obtained from the careful solution of a three-dimensional Patterson map; the solution of the Patterson function was complicated by the pseudospecial positioning of the Cr atom and the ionic chloride atoms (related by $\sim a/2$, Table III). The remaining nonhydrogen atoms were obtained from a difference Fourier synthesis following the first structure factor calculation. Refinement of scale factor and positional and isotropic thermal parameters for all atoms²² converged at $R = 0.088$ for the 1723-reflection data set. At this point, each atom was assigned individual anisotropic temperature factors (suggested by features on a difference map) and refinement converged to $R = 0.057$ and $R_w = 0.076$. The weights used in refinement were $w = [\sigma^2(F_o) + (0.035|F_o|)^2]^{-1}$. A difference Fourier synthesis at this point revealed the positions of the 25 hydrogen atoms. Further refinement of all 39 atoms, with positional and isotropic thermal parameters varied for all hydrogen atoms, resulted in convergence, with $R = 0.039$ and $R_w = 0.051$ (observation:parameters = 7.6:1). At this point it was decided to refine as above, but to include all 2365 data in the refinement; at convergence $R = 0.061$ and $R_w = 0.057$ (observations:parameters = 10.4:1). On the final cycle of least-squares refinement, no individual parameter shift was greater than 0.1 of the corresponding esd. Parameters based on the 2365 reflection data set were not significantly different either (a) from those based on the 1723-reflection data set or (b) from a 2365-reflection data set where weak reflections were treated as described by Churchill.²³ The parameter set using 2365 reflections in either case had esd's which were 10–15% lower than the parameter set using 1723 reflections. Further justification for inclusion of ~ 650 weak reflections in this fairly small data set is the unusual distribution of reflections due to pseudosymmetry. For the eight parity groups, values of mean E^2 are the following: eee, 1.478; eeo, 0.544; eoe, 1.497; eoo, 0.556; oee, 1.241; oeo, 0.568; ooe, 1.419; ooo, 0.396. A final difference Fourier map showed peaks of 0.4–0.5 $e/\text{\AA}^3$ near the Cl atoms and no other maxima greater than 0.3 $e/\text{\AA}^3$. Corrections for absorption ($\mu = 13.7 \text{ cm}^{-1}$) or extinction were not made. A weighting scheme analysis revealed no serious dependence of $w[|F_o| - |F_c|]^2$ on $|F_o|$, $(\sin \theta)/\lambda$, indices, or parity groups. The standard deviation of an observation of unit weight is 1.03 ($m = 2365$, $n = 227$). Final atomic coordinates and thermal parameters, together with their estimated standard deviations are listed in Tables III and IV, respectively.

Results and Discussion

The structures of the $\text{M}(\text{NH}_2\text{R})_5\text{Cl}^{2+}$ molecular cations oriented in the same manner are presented in Figure 1. Two salient features of the structural chemistry are apparent from these drawings.²⁴ (a) The methylamine ligands are in a staggered conformation; thus, despite severe steric interactions (vide infra), the "normal" ligand conformation is observed. (b) The ligand configurations about both Co and Cr are rather similar. In particular, the disposition of Cl and ligands 1, 4, and 5 is very similar in both complexes, while ligands 2 and 3 are disposed differently.

While it is interesting to note these similarities, it is of much greater importance to establish the details of how, why, and where the complexes differ and the relationship of this dif-

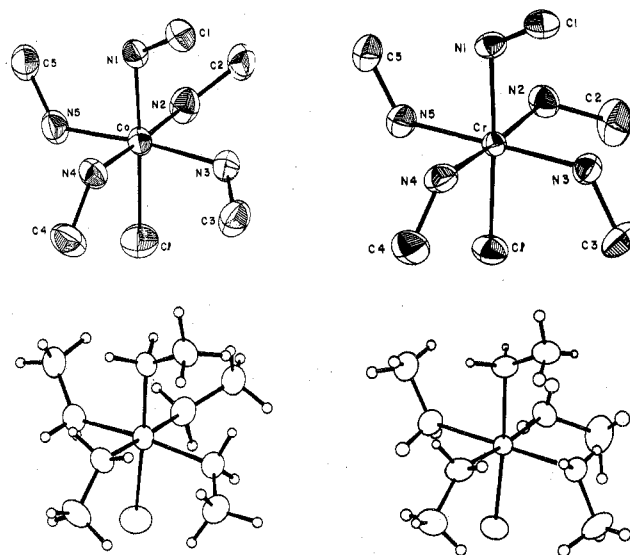


Figure 1. Molecular structures of $\text{Co}(\text{NH}_2\text{CH}_3)_5\text{Cl}^{2+}$ and $\text{Cr}(\text{NH}_2\text{CH}_3)_5\text{Cl}^{2+}$, showing 50% probability ellipsoids and methylamine hydrogen atoms.

ference to solution-chemical behavior.

Bond Lengths and Angles. The M–N bond lengths (Table V) are within the ranges observed for Co(III)– and Cr(III)– NH_2R where R = alkyl;²⁵ other bond lengths are also normal. However, inspection of the angles subtended at the metal and at the amine nitrogen atoms reveals that there are very large distortions, reaching maxima of 6.6 and 15° from expected octahedral and tetrahedral values, respectively. Thus, despite the fact that the Cr–N bond lengths are $\sim 0.1 \text{ \AA}$ longer than the Co–N bond lengths, both complexes show rather similar angle distortions (Table V). On the basis of these distortions, it is not possible to ascertain which complex is the more highly strained; however, such information is readily obtained from inspection of nonbonded contacts $\leq 3.5 \text{ \AA}$ (Table VI). It is seen that, in general, the nonbonded contacts for the cobalt complex are 0.1–0.2 \AA shorter than the corresponding contacts for the chromium complex. Further, there are five fewer contacts $< 3.5 \text{ \AA}$ in the chromium complex. Thus, a pattern emerges here similar to that observed in Co(III) chelate complexes: nonbonded interactions are minimized by appropriate bond angle distortions and/or torsion about Co–N and N–C (and C–C) bonds.²⁶ In general, studies of strain in Co(III) chelate complexes have emphasized the thermodynamic rather than kinetic stability of the complex ions.

Angle Deformations in Alkylamine Complexes. It is of interest to consider M–N–C angle distortions in alkyl-amine complexes in a general sense. The two complexes discussed in this paper differ in the extent of severity of their intra-

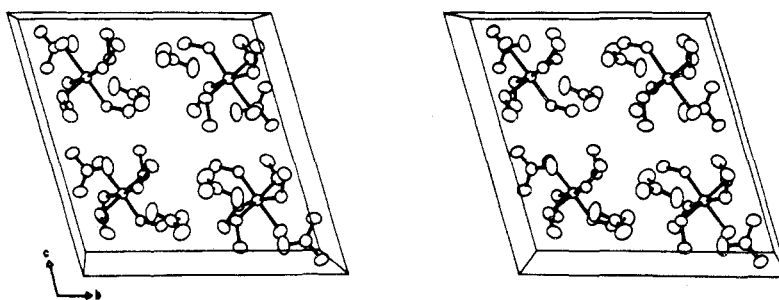
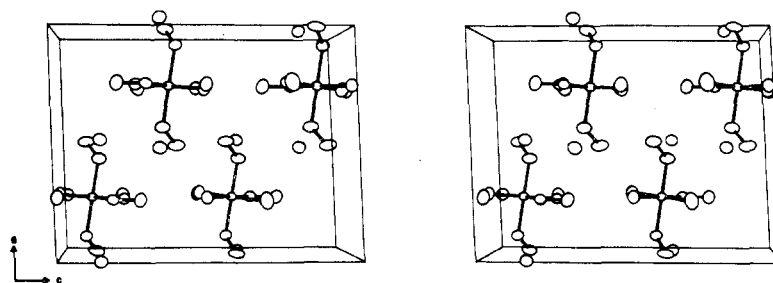
Figure 2. Stereoscopic view of the unit cell of $[\text{Co}(\text{NH}_2\text{CH}_3)_5\text{Cl}](\text{NO}_3)_2$.Figure 3. Stereoscopic view of the unit cell of $[\text{Cr}(\text{NH}_2\text{CH}_3)_5\text{Cl}]\text{Cl}_2$.

Table V. Distances (Å) and Angles (deg)

(a) For $\text{M}(\text{NH}_2\text{CH}_3)_5\text{Cl}^{2+}$ Ions ^a					
Bond	M = Cr	M = Co	Bond	M = Cr	M = Co
M-N1	2.103 (4)	1.980 (3)	N1-C1	1.461 (6)	1.466 (6)
M-N2	2.094 (4)	1.998 (4)	N2-C2	1.450 (7)	1.479 (6)
M-N3	2.105 (4)	1.991 (4)	N3-C3	1.488 (6)	1.483 (6)
M-N4	2.091 (4)	1.979 (3)	N4-C4	1.457 (7)	1.482 (6)
M-N5	2.099 (5)	1.994 (4)	N5-C5	1.472 (6)	1.475 (6)
M-Cl	2.299 (1)	2.283 (1)	N-H (wtd av)	0.87 (2)	
			C-H (wtd av)	0.94 (2)	
Angle	M = Cr	M = Co	Angle	M = Cr	M = Co
M-N1-C1	121.8 (3)	120.7 (3)	N2-M-N3	94.6 (2)	87.9 (1)
M-N2-C2	120.5 (3)	122.8 (3)	N2-M-N4	175.4 (2)	177.6 (2)
M-N3-C3	121.3 (3)	121.8 (3)	N2-M-N5	86.4 (2)	89.2 (1)
M-N4-C4	121.7 (3)	123.7 (3)	N2-M-Cl	88.7 (1)	87.3 (1)
M-N5-C5	124.5 (3)	124.5 (3)	N3-M-N4	87.5 (2)	93.5 (1)
N1-M-N2	89.8 (2)	91.7 (1)	N3-M-N5	178.9 (2)	171.7 (1)
N1-M-N3	91.2 (2)	96.6 (1)	N3-M-Cl	93.9 (1)	86.9 (1)
N1-M-N4	86.0 (2)	86.2 (1)	N4-M-N5	91.5 (2)	89.7 (1)
N1-M-N5	89.5 (2)	91.2 (1)	N4-M-Cl	95.3 (1)	94.7 (1)
N1-M-Cl	174.8 (1)	176.3 (1)	N5-M-Cl	85.5 (1)	85.2 (1)

(b) Nitrate Anions in $[\text{Co}(\text{NH}_2\text{CH}_3)_5\text{Cl}](\text{NO}_3)_2$

Bond	Angle
N6-O1	1.222 (5)
N6-O2	1.241 (5)
N6-O3	1.242 (5)
N7-O4	1.247 (5)
N7-O5	1.224 (5)
N7-O6	1.253 (5)
O1-N6-O2	120.5 (4)
O1-N6-O3	120.2 (4)
O2-N6-O3	119.3 (4)
O4-N7-O5	120.4 (4)
O4-N7-O6	118.9 (4)
O5-N7-O6	120.7 (4)

^a In this table and in Table VI, "Cl" refers to Cl1 for $\text{Cr}(\text{NH}_2\text{CH}_3)_5\text{Cl}^{2+}$.

molecular nonbonded interactions; however, the M-N-C angular distortions are similar. This suggests that, in the chromium complex (the *less* strained complex), a *limiting value has been reached for M-N-C distortions*. Some insight into the "distortability" of M-N-C angles can be gained from inspection of Table VII. We note that four-coordinate complexes, in general, show much smaller distortions than six-coordinate complexes, an obvious consequence of fewer nonbonded interactions. The list of complexes available for comparison is regrettably short; however, the relative ease of M-N-C angle deformation, as well as the differences evident

Table VI. Intramolecular Nonbonded Contacts (<3.5 Å) in $\text{M}(\text{NH}_2\text{CH}_3)_5\text{Cl}^{2+}$

Atom pair	M = Cr	M = Co	Atom pair	M = Cr	M = Co
Cl-N2	3.073	2.961	C1-N3	3.043	3.068
Cl-N3	3.220	2.947	C1-N4		3.366
Cl-N4	3.247	3.142	N2-N3	3.085	2.769
Cl-N5	2.989	2.903	N2-N5	2.870	2.802
Cl-C3	3.205	3.437	N2-C5		3.443
Cl-C4	3.247	3.166	C2-N3	3.189	3.099
			N3-N4	2.902	2.892
N1-N2	2.964	2.854	C3-N4		3.055
N1-C2		3.225	C3-C4		3.466
N1-N3	3.006	2.965	N4-N5	3.002	2.801
N1-N4	2.861	2.706			
N1-N5	2.957	2.839			
N1-C5	3.053	3.014			

Table VII. M-N-C Angles (deg) in Various Complexes

Complex	M-N-C angle(s)	Ref
$\text{Mn}(\text{CO})_4(\text{NH}_2\text{CH}_3)(\text{CONHCH}_3)$ (2 forms)	118.9 (10), 121.1 (7)	27
$\text{Pt}(\text{NH}_2\text{CH}_3)_4^{2+}$	123 (?)	28
$\text{Pt}(\text{NH}_2\text{CH}_2\text{CH}_3)_4^{2+}$	112 (5)	28
$[\text{Re}(\text{NH}_2\text{CH}_3)_4(\text{NCH}_3)\text{Cl}]^{2+}$	119 (1), 119 (1), 125 (1), 122 (1)	29
<i>trans</i> - $\text{Pt}(\text{NH}_3)_2(\text{NH}(\text{CH}_3)_2)_2^{2+}$	113.1 (8), 117.0 (15)	30

between four- and six-coordination, is established.

Crystal Structures. The packing of the Co and Cr complexes is shown in Figures 2 and 3, respectively. Both complexes are extensively hydrogen bonded, as indicated in Table VIII. In the Co structure, the nitrate anions have two longer and one shorter distance (Table V); further, in each anion, the O-N-O angle associated with the longer two N-O distances is less than 120° . While these features are just barely significant, they are probably real; Table VIII indicates that H-bonding interactions to atoms O1 and O5 are relatively weak.

Summary and Conclusions

If this structural work is reviewed in the light of recent mechanistic studies, it is found that the structural results correlate rather well with the solution chemistry.

(1) Both the Co and Cr complexes have severely crowded ground-state structures; on the basis of nonbonded interactions it may be concluded that the Co complex is more highly

Table VIII. Intermolecular Contacts (<3.9 Å) Involving Probable Hydrogen Bonds

Atoms	Distance, Å	Angle X-H...Y, deg	Symmetry operation
(a) [Cr(NH ₂ CH ₃) ₅ Cl]Cl ₂			
N1-Cl3	3.416	161.7	x, y, z
N1-Cl2	3.498	171.0	x, y, z
N2-Cl3	3.421	153.0	$\bar{x}, 1-y, \bar{z}$
N2-Cl3	3.308	150.4	x, y, z
N3-Cl3	3.406	160.7	$\bar{x}, y-1/2, 1/2-z$
N3-Cl2	3.364	161.1	$1-x, y-1/2, 1/2-z$
N4-Cl2	3.391	164.9	$1-x, y-1/2, 1/2-z$
N4-Cl2	3.281	163.0	x, y, z
N5-Cl3	3.413	155.3	$\bar{x}, 1-y, \bar{z}$
N5-Cl2	3.433	149.0	$1-x, 1-y, \bar{z}$
(b) [Co(NH ₂ CH ₃) ₅ Cl](NO ₃) ₂			
N1-O6	3.186	169.4	$x-1/2, y, z-1/2$
N1-O1	3.123	140.4	$x-1, y, z$
N2-O4	3.163	141.2	x, y, z
N2-O6	3.149	155.4	$1/2-x, \bar{y}, 1/2-z$
N3-O5	3.184	147.9	x, y, z
N4-O2	3.107	158.9	$1/2-x, 1-y, 1/2-z$
N4-O3	2.968	178.8	$x-1, y, z$
N5-O4	3.091	153.8	$1/2-x, \bar{y}, 1/2-z$
C5-O6	3.282	153.0	$x-1/2, y, z-1/2$
C5-O3	3.248	135.3	$x-1, y, z$

Table IX. Rates of Substitution Reactions for MA₅Cl²⁺ Complexes

Complex	Process, probable mechanism	Rate	Ref
Co(NH ₃) ₅ Cl ²⁺	Acid hydrolysis, I _d	$1.7 \times 10^{-6} \text{ s}^{-1}$	31
Co(NH ₂ CH ₃) ₅ Cl ²⁺	Acid hydrolysis, I _d	$37 \times 10^{-6} \text{ s}^{-1}$	32
Co(NH ₃) ₅ Cl ²⁺	Base hydrolysis, D _{cb}	$0.25 \text{ M}^{-1} \text{ s}^{-1}$	33
Co(NH ₂ CH ₃) ₅ Cl ²⁺	Base hydrolysis, D _{cb}	$3800 \text{ M}^{-1} \text{ s}^{-1}$	4
Cr(NH ₃) ₅ Cl ²⁺	Acid hydrolysis, I _d	$8.7 \times 10^{-6} \text{ s}^{-1}$	3
Cr(NH ₂ CH ₃) ₅ Cl ²⁺	Acid hydrolysis, I _d	$0.26 \times 10^{-6} \text{ s}^{-1}$	3
Cr(NH ₃) ₅ Cl ²⁺	Base hydrolysis, D _{cb}	$1.92 \times 10^{-3} \text{ M}^{-1} \text{ s}^{-1}$	3
Cr(NH ₂ CH ₃) ₅ Cl ²⁺	Base hydrolysis, D _{cb}	$4.32 \times 10^{-1} \text{ M}^{-1} \text{ s}^{-1}$	3

strained. This crowding may be expected to lead to kinetic steric effects in octahedral substitution reactions, viz., *steric acceleration* in a D or I_d process where relief of strain is achieved in the activated complex or *steric retardation* in an A or I_a process where strain is expected to increase in the activated complex. Inspection of Table IX shows this to be the case; for each pair, the replacement of NH₃ by NH₂CH₃ shows the appropriate kinetic steric effect. Further, for the base hydrolysis reaction, the acceleratory effect is much greater for M = Co, in agreement with the more severe nonbonded interactions observed. Since Co(III) has the smallest radius of all trivalent transition metal ions, it is *most likely* to show kinetic steric effects; it is thus an inappropriate metal ion for selection as a model for general octahedral substitution.^{6b}

(2) In Cr(III) chemistry, loss of ammine or amine ligands is not unusual; in Co(III) chemistry such loss is relatively rare. However, in the Co(RNH₂)₅Cl²⁺ system, such loss has been observed and has been further characterized to be the loss of an amine trans to the hydroxo ligand in Co(RNH₂)₅OH²⁺, producing *trans*-Co(RNH₂)₄(OH)₂⁺.³⁴ This process occurs at a pH-independent rate⁴ of $\sim 2 \times 10^{-4} \text{ s}^{-1}$ and may be an "accelerated" version of *ammine* ligand loss in Co(NH₃)₅OH²⁺,³⁵ further investigation of that reaction with the above information in hand might be informative.

(3) Finally, we feel that it is pertinent to conclude with speculation on the existence of octahedral, monodentate secondary amine complexes (of the type discussed here) in the first transition series. Such complexes would be interesting not only for steric reasons but also from the viewpoint of study of racemization at unchelated centers. Attempts to prepare

pentakis(isopropylamine)halometal(III) ions inevitably fail,³⁶ although Co(en)₂(i-C₃H₇NH₂)Cl²⁺ is known.³⁷ To date no pure monodentate secondary amine complexes even as simple as (R₂NH)(NH₃)₄MCl²⁺ (M = Co, Cr) are known. Clearly, the difficulty of preparation is a likely consequence of severe steric crowding; undoubtedly, the presence of such a species in the metal's coordination sphere is more likely to lead to labile complexes of the type MX₃·2L³⁸ than to the desired inert six-coordinate species.

Acknowledgment. We thank the Australian National University for generous allocations of computer time. This work was supported by the donors of the Petroleum Research Fund, administered by the American Chemical Society, and the National Science Foundation, through Instrumentation Grant CHE 76-05582.

Registry No. [Co(NH₂CH₃)₅Cl](NO₃)₂, 18890-70-5; [Cr(NH₂CH₃)₅Cl]Cl₂, 15351-84-5.

Supplementary Material Available: Listings of observed and calculated structure factor amplitudes (Tables X and XI) (17 pages). Ordering information is given on any current masthead page.

References and Notes

- (1) Address correspondence to Brandeis University.
- (2) For a review, see M. L. Tobe, *Acc. Chem. Res.*, **3**, 377 (1970).
- (3) M. Parris and W. J. Wallace, *Can. J. Chem.*, **47**, 2257 (1969).
- (4) D. A. Buckingham, B. M. Foxman, and A. M. Sargeson, *Inorg. Chem.*, **9**, 1790 (1970).
- (5) B. M. Foxman, *J. Chem. Soc., Chem. Commun.*, 515 (1972).
- (6) (a) G. Guastalla and T. W. Swaddle, *Can. J. Chem.*, **51**, 821 (1973); (b) S. B. Tong and T. W. Swaddle, *Inorg. Chem.*, **13**, 1538 (1974); (c) T. W. Swaddle, *Coord. Chem. Rev.*, **14**, 217 (1974).
- (7) Equivalent positions: $\pm(x, y, z)$; $\pm(1/2+x, y, 1/2+z)$.
- (8) The Busing and Levy programs (*Acta Crystallogr.*, **22**, 457 (1967)), as modified by Picker Corp., were used for all phases of diffractometer control.
- (9) A. L. Beauchamp, M. J. Bennett, and F. A. Cotton, *J. Am. Chem. Soc.*, **90**, 6675 (1968).
- (10) All programs used here have been described in detail previously: G. B. Robertson and P. O. Whimp, *Inorg. Chem.*, **12**, 1740 (1973); **13**, 1047 (1974). Additionally, the program CONTACT by J. F. Blount was used to generate tetrahedral hydrogen atom positions.
- (11) W. R. Busing and H. A. Levy, *J. Chem. Phys.*, **26**, 563 (1957); P. W. R. Corfield, R. J. Doedens, and J. A. Ibers, *Inorg. Chem.*, **6**, 197 (1967).
- (12) Throughout the refinement, the function minimized was $\sum w(|F_o| - |F_c|)^2$ where $|F_o|$ and $|F_c|$ are the observed and calculated structure amplitudes and w is the weight. The agreement indices are defined as $R = \sum(|F_o| - |F_c|) / \sum |F_o|$ and $R_w = \{\sum w(|F_o| - |F_c|)^2 / \sum w |F_o|^2\}^{1/2}$. Scattering factors: for Co and Cl, from D. T. Cromer and J. T. Waber, *Acta Crystallogr.*, **18**, 104 (1965); for H, from R. P. Stewart, E. R. Davidson, and W. T. Simpson, *J. Chem. Phys.*, **42**, 3175 (1965); for remaining atoms, from "International Tables for X-Ray Crystallography", Vol. 3, The Kynoch Press, Birmingham, England, 1962, pp 202-203.
- (13) J. S. Rollet, Ed., "Computing Methods in Crystallography", Pergamon Press, Oxford, England, 1965, p 50.
- (14) (a) C. T. Prewitt, Ph.D. Thesis, Massachusetts Institute of Technology, 1962, p 163; (b) D. T. Cromer, *Acta Crystallogr.*, **18**, 17 (1965).
- (15) Since it was thought at this stage that the positions would be used to calculate the magnitude of nonbonded interactions, the spectroscopic values were used rather than more appropriate values: M. R. Churchill, *Inorg. Chem.*, **12**, 1213 (1973).
- (16) W. A. Zachariasen, *Acta Crystallogr.*, **16**, 1139 (1963).
- (17) A. Rogers and P. J. Staples, *J. Chem. Soc.*, 6834 (1965).
- (18) R. A. Sparks et al., "Operations Manual, Syntex P2, Diffractometer", Syntex Analytical Instruments, Cupertino, Calif., 1972.
- (19) E. J. Brooker and E. W. Nuffield, *Acta Crystallogr.*, **20**, 496 (1966).
- (20) "International Tables for X-Ray Crystallography", Vol. 3, The Kynoch Press, Birmingham, England, 1962, p 122.
- (21) R. A. Sparks et al., "Operations Manual, Syntex XTL Structure Determination System", Syntex Analytical Instruments, Cupertino, Calif., 1976. Minor local modifications have been made to most of the programs, e.g., a test for positive definiteness of temperature factors was added. Other programs used on our system include: SYNFUL, structure factor tables (B.M.F.); PARM, data file manipulation, and ESD, table preparation, from Professor I. C. Paul's group, University of Illinois.
- (22) Scattering factors and anomalous scattering corrections are those given in "International Tables for X-Ray Crystallography", Vol. IV, The Kynoch Press, Birmingham, England, 1974, pp 99-101, 148-150.
- (23) M. R. Churchill, *Inorg. Chem.*, **12**, 1213 (1973).
- (24) Drawings are all retouched Versatec D1100A output from the Syntex XTL version of ORTEP by C. K. Johnson and program ORTIN by Syntex programming staff.
- (25) See (a) F. A. Jurnak and K. N. Raymond, *Inorg. Chem.*, **13**, 2387 (1974), and references therein; (b) E. N. Duesler and K. N. Raymond, *ibid.*,

- 10, 1486 (1971), for examples. Both sets of M-N distances are among the longest reported.
- (26) D. A. Buckingham and A. M. Sargeson, *Top. Stereochem.*, **6**, 219 (1971); B. F. Anderson, J. D. Bell, D. A. Buckingham, P. J. Creswell, G. J. Gainsford, L. G. Marzilli, G. B. Robertson, and A. M. Sargeson, *Inorg. Chem.*, **16**, 3233 (1977), and references therein.
- (27) D. M. Chipman and R. A. Jacobson, *Inorg. Chim. Acta*, **1**, 393 (1967); G. L. Breneman, D. M. Chipman, C. J. Galles, and R. A. Jacobson, *Inorg. Chim. Acta*, **3**, 447 (1969).
- (28) M. E. Cradwick, D. Hall, and R. K. Phillips, *Acta Crystallogr., Sect. B*, **27**, 480 (1971).
- (29) R. S. Shandles, R. K. Murmann, and E. O. Schlemper, *Inorg. Chem.*, **13**, 1373 (1974).
- (30) J. S. Anderson, J. W. Carmichael, and A. W. Cordes, *Inorg. Chem.*, **9**, 143 (1970).
- (31) F. J. Garrick, *Trans. Faraday Soc.*, **33**, 486 (1937).
- (32) M. Parris, *J. Chem. Soc. A*, 583 (1967).
- (33) D. A. Buckingham, I. I. Olsen, and A. M. Sargeson, *Inorg. Chem.*, **7**, 174 (1968).
- (34) M. Raider and B. M. Foxman, unpublished observations; this loss has also been observed in pH titration of $(\text{CH}_3\text{NH}_2)_5\text{CoOH}_2^{3+}$: T. W. Swaddle, *Can. J. Chem.*, **55**, 3166 (1977).
- (35) J. Bjerrum, "Metal Ammine Formation in Aqueous Solution", P. Hasse and Son, Copenhagen, 1957, Chapter XI; for a further example, see A. M. Newton and T. W. Swaddle, *Can. J. Chem.*, **52**, 2751 (1974).
- (36) B. M. Foxman, unpublished observations. This discussion excludes complexes of the relatively constrained ligand ethyleneimine, which may be prepared with $\text{CoA}_2\text{X}^{2+}$ stoichiometry.
- (37) S. C. Chan and S. F. Chan, *J. Chem. Soc. A*, 202 (1969).
- (38) Examples: G. W. A. Fowles, P. T. Greene, and J. S. Wood, *Chem. Commun.*, 971 (1967); B. J. Russ and J. S. Wood, *ibid.*, 745 (1966).

Contribution from the Laboratory for Crystallography,
University of Amsterdam, Amsterdam, The Netherlands

Bis(μ -trifluoroacetato-*O, O'*)-bis[dimethyl(4-methylpyridine)platinum](Pt-Pt)

J. D. SCHAGEN, A. R. OVERBEEK, and H. SCHENK*

Received October 27, 1977

The crystal structure of the title compound has been determined from 1921 independent nonzero reflections collected with a Nonius CAD4 diffractometer using $\text{Cu K}\alpha$ radiation. The compound crystallizes in the orthorhombic space group $P2_12_12_1$ with cell constants $a = 8.854$ (1) Å, $b = 15.334$ (2) Å, $c = 18.967$ (2) Å, and $Z = 4$. The structure was solved by Patterson and Fourier methods and refined to an R value of 4.9%. The Pt(1)-Pt(2) distance of 2.557 (1) Å is one of the shortest known bridged Pt-Pt bonds. The platinum atoms are octahedrally surrounded by the ligands. As a result of steric interaction between the methyl groups the octahedra are slightly deformed and rotated by 23° with respect to each other. The angles Pt-Pt-N are 169° .

Introduction

Binuclear compounds containing metal-metal bonds bridged by carboxylato groups,¹⁻⁴ triazenido groups,⁵⁻⁹ and amidino groups^{1,6,7,10-13} are receiving great interest lately. Best known are compounds containing quadruple metal-metal bonds¹⁰⁻¹³ which are abundant for the complexes of metals of the Cr triad.

Recently, reports have appeared on the formation of Pt-Pt bonded compounds bridged by biphosphines,¹⁹ sulfate groups,¹⁴ $\text{P}_2\text{O}_7^{4-}$ groups,¹⁵ α -pyridonato groups,¹⁶ and carboxylato groups.^{17,18}

Of particular interest are compounds of the type $[\text{cis-R}_2\text{Pt}(\text{O}_2\text{CR}')\text{L}]_2$ ($\text{R} = \text{alkyl, aryl}$)^{17,18} and the asymmetrical complexes $\text{Pt}_2\text{R}_4(\text{O}_2\text{CR}')_2\text{L}^{18}$ in which one formally trivalent Pt(III) is six-coordinated and the other Pt(III) is five-coordinated.

In order to determine the influence of the bridging groups and of the number of L groups on the structure of the complexes and on the metal-metal bond length, a crystallographic study was undertaken of $[\text{Me}_2\text{Pt}(\text{O}_2\text{CCF}_3)(4\text{-Me-py})]_2$, the results of which are given here, and recently we started an investigation of $[\text{Ph}_4\text{Pt}_2(\text{O}_2\text{CCH}_3)_2(\text{PEt}_3)]$.

Experimental Section

Weissenberg photographs suggested an orthorhombic space group and the systematic absences of $h00$ for $h = 2n + 1$, $0k0$ for $k = 2n + 1$ and $00l$ for $l = 2n + 1$ indicated space group $P2_12_12_1$.

Unit cell dimensions determined on an Enraf-Nonius CAD4 diffractometer using graphite-monochromated $\text{Cu K}\alpha$ radiation and a θ - 2θ scan are $a = 8.854$ (1) Å, $b = 15.334$ (2) Å, $c = 18.967$ (2) Å, and $Z = 4$.

For the intensity measurements an approximately spherical crystal was selected. A total of 1921 independent nonzero reflections were collected in the range $2 < \theta < 60^\circ$, 1798 of which were above the significance level of 2.5σ . Experimental data were corrected for absorption using the factors for a sphere²⁰ with $r = 0.09$ mm ($\mu =$

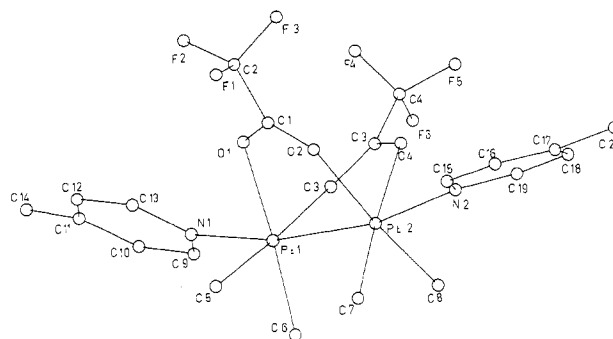


Figure 1. Molecular structure of $\text{Pt}_2(\text{O}_2\text{C}_2\text{F}_3)_2(\text{CH}_3)_4(\text{NC}_6\text{H}_7)_2$ and numbering of the atoms.

203.97 cm^{-1}). Judging from the real dimensions of the crystal ($0.176 \times 0.180 \times 0.184$ mm) the systematic error not accounted for by this approximation is small.

Structure Determination and Refinement

The positions of the platinum atoms were found from a sharpened Patterson function; the other nonhydrogen atoms were located in a difference Fourier synthesis. No attempt was made to locate hydrogen atoms. The refinement has been carried out by means of a block-diagonal least-squares procedure, using anisotropic temperature factors for the platinum atoms, isotropic factors for the rest of the atoms, and a Cruickshank weighting scheme. The final R value was 4.9%, and refinement of the enantiomorph resulted in an R value of 5.6%. The large thermal parameters of the F atoms suggest disorder of the CF_3 groups, a common phenomenon for these groups. The presence of disorder was confirmed in a difference synthesis; however, the information was not accurate enough to include it in the refinement.

Results and Description of the Structure

The molecular structure of $\text{Pt}_2(\text{O}_2\text{C}_2\text{F}_3)_2(\text{CH}_3)_4(\text{NC}_6\text{H}_7)_2$ is depicted in Figure 1, which also gives the numbering scheme. A stereoscopic view is given in Figure 2 and a Newman